

# Magnetoencephalographic Imaging

Srikantan Nagarajan and Kensuke Sekihara

**Abstract** Non-invasive and dynamic imaging of brain activity in the sub-millisecond time-scale is enabled by measurements on or near the scalp surface using an array of sensors that measure magnetic fields (magnetoencephalography (MEG)) or electric potentials (electroencephalography (EEG)). Algorithmic reconstruction of brain activity from MEG data is referred to as magnetoencephalographic imaging (MEGI). Reconstructing the actual brain response to external events and distinguishing unrelated brain activity has been a challenge for many existing algorithms in this field. Furthermore, even under conditions where there is very little interference, accurately determining the spatial locations and timing of brain sources from MEG data is a challenging problem because it involves solving for unknown brain activity across thousands of voxels from just a few sensors ( $\sim 300$ ). In recent years, our research group has developed a suite of novel and powerful algorithms for MEGI that we have shown to be considerably superior to existing benchmark algorithms. Specifically, these algorithms can solve for many brain sources, including sources located far from the sensors, in the presence of large interference from unrelated brain sources. Our algorithms efficiently model interference contributions to sensors, accurately estimate sparse brain source activity using fast and robust probabilistic inference techniques. Here, we review some of these algorithms and illustrate their performance in simulations and real MEG/EEG data. We also briefly how functional connectivity approaches have evolved and are being applied in conjunction with MEG imaging.

**Keywords** MEG · EEG · Source reconstruction · Forward models · Inverse algorithms · Bayesian methods · Functional connectivity · Group statistics

---

S. Nagarajan (✉)

Department of Radiology and Biomedical Imaging, University of California,  
513 Parnassus Avenue, S362, San Francisco, CA 94143, USA  
e-mail: sri@ucsf.edu

K. Sekihara

Department of Systems Design & Engineering, Tokyo Metropolitan University,  
Asahigaoka 6-6, Hino, Tokyo 191-0065, Japan

## 1 Introduction

Multiple modalities of non-invasive functional brain imaging have made a tremendous impact in improving our understanding of human auditory cortex. Ever since its advent in 1991, functional magnetic resonance imaging (fMRI) has emerged as the predominant modality for imaging of the functioning brain, for several reasons (Belliveau et al. 1992; Ogawa et al. 1992; Tank et al. 1992). fMRI uses MRI to measure changes in blood oxygenation level-dependent (BOLD) signals due to neuronal activation. It is a safe, non-invasive method that allows for whole-brain coverage, including the ability to examine activity in deep brain structures. Importantly, the widespread availability of commercial and open-source tools for analysis of fMRI data has enabled many researchers to easily embrace this technology. However, since the BOLD signal is only an indirect measure of neural activity and is fundamentally limited by the rate of oxygen consumption and subsequent blood flow mechanism, fMRI lacks the temporal resolution required to image the dynamic and oscillatory spatiotemporal patterns that are associated with cognitive processes. The temporal resolution limitations of fMRI particularly constrain auditory studies because auditory stimuli and responses have inherently fast dynamics that cannot be readily assessed with fMRI. Furthermore, since the BOLD signal is only an approximate, indirect measure of neural activity, it might not accurately reflect true neuronal processes especially in regions of altered vasculature. In fact the exact frequency-band of neuronal processes that corresponds to the BOLD signal is still being actively debated (Logothetis et al. 2001; Niessing et al. 2005). Finally, in the context of auditory studies of speech and language, because fMRI measurements involve loud scans, caused by fast forces on MR gradient coils, the scans themselves will invoke auditory responses that have to be deconvolved from the signals in order to examine external stimulus related activity. Hence, to non-invasively image brain activity on a neurophysiologically relevant timescale and to observe neurophysiological processes more directly, silent imaging techniques are needed that have both high temporal and adequate spatial resolution.

Temporal changes can be non-invasively measured using methods with high (e.g. millisecond) temporal resolution, namely magnetoencephalography (MEG) and electroencephalography (EEG). MEG measures tiny magnetic fields outside of the head that are generated by neural activity. EEG is the measurement of electric potentials generated by neural activity using an electrode array placed directly on the scalp. In contrast to fMRI, both MEG and EEG directly measure electromagnetic (EM) fields emanating from the brain with excellent temporal resolution ( $<1$  ms) and allow the study of neural oscillatory processes over a wide frequency range (at least 1–600 Hz). MEG and EEG also provide complementary information about brain activity because of their differing sensitivity to current sources within the brain. While MEG is primarily sensitive to tangential currents in the brain closer to the surface and insensitive to poor conductive properties of the skull, EEG is primarily sensitive to radial sources while being highly sensitive to

the conductive properties of the brain, skull, and scalp. Since bioelectric currents produced by neurons also generate magnetic fields, which are not distorted by the heterogeneous environment, measurements of these magnetic fields using MEG can be considered to give rise to an undistorted signature of underlying cortical activity. Therefore, MEG and EEG can be viewed as being complementary in terms of the sensitivity to underlying neural activity. In this chapter, a review is initially presented on how brain activity can be reconstructed from MEG measurements with implications for spatial and temporal resolution of such reconstructions.

## 2 Sensing the Brain's Magnetic Fields

Biomagnetic fields detected by MEG are extremely small, in the tens-to-hundreds of femto-Tesla (fT) range—seven orders of magnitude smaller than the earth's magnetic field, and as a result, appropriate data collection necessitates a magnetically shielded room and highly sensitive detectors—Superconducting quantum interference devices (SQUIDS). The fortuitous anatomical arrangement of cortical pyramidal cells allows the noninvasive detection of their activity by MEG. The long apical dendrites of these cells are arranged perpendicularly to the cortical surface and parallel to each other, allowing their electromagnetic fields to often sum up to magnitudes large enough to detect at the scalp. Synchronously fluctuating dendritic currents result in electric and magnetic dipoles that produce these electromagnetic fields (Nunez and Srinivasan 2006). These dendritic currents from the brain are typically sensed using detection coils called flux transformers or magnetometers, which are positioned closely to the scalp and connected to SQUIDS. SQUIDS act as a magnetic-field-to-voltage converter, and its typically non-linear response is linearized by flux-locked loop electronic circuits, and have a sensitivity of  $\sim 10$  femto-Tesla per square root of Hz which is adequate for detection of brain's magnetic fields (Vrba and Robinson 2002).

MEG sensors are often configured for differential magnetic field measurements to reduce ambient noise in measurements—which are also referred to as gradiometers, although some MEG systems are also built out of magnetometers and rely on magnetic shielding and clever electronics for noise cancellation. The two commonly used gradiometer configurations are axial and planar gradiometers. Axial gradiometers consist of two coils that share an axis, whereas planar gradiometers measure gradients (or differences) of magnetic fields in a given plane. The sensitivity profile of planar gradiometer sensors is somewhat similar to EEG, whereby a sensor is maximally sensitive to a source closest to it on the cortical surface. In contrast however, the sensitivity profile of an axial gradiometer can be somewhat counterintuitive because it is not maximally sensitive to sources closest to the sensors. Both planar and axial gradiometers are sensitive to the orientation of the sources in a counterintuitive manner, similar to EEG sensors.

Modern MEG systems often consist of simultaneous recordings from many differential sensors that cover the whole head, and the total number of sensors varies from 100–300. The advent of such array systems has significantly advanced MEG studies. Typical MEG systems have sensors that are spaced approximately 2.2–3.6 cm apart. Although the maximum sampling rate for many MEG systems is approximately 12 kHz, most MEG data is usually recorded at about 1,000 Hz, thereby still providing excellent temporal resolution for measuring the dynamics of cortical neuronal activity at the millisecond level.

There are many reasons why neuroscientists have embraced MEG. First, MEG setup time is very short and convenient for both experimenters and subjects. A participant or patient can be in the scanner within 10–15 min from entering the laboratory because—unlike EEG—the lengthy time necessary to apply and check electrodes is obviated. Second, the anatomical location of large parts of primary sensory cortices in sulci makes MEG ideally suited for electrophysiological studies in audition. Furthermore, with whole-head sensor arrays, MEG is also well-suited to investigate hemispheric lateralization effects based on sensor waveforms. In contrast to evoked responses measured with EEG, which are maximal at midline electrodes making hemispheric effects difficult to characterize, MEG responses are well lateralized. Distinct groups of MEG sensors are sensitive to lateralized temporal lobe activity that allows for hemisphere-specific assessments.

### **3 From Sensing to Imaging: The Prerequisites**

MEG sensor data analysis only provides qualitative information about underlying brain regions whose activity is observed on the sensor array based on experienced users' intuitions about the sensitivity profile of the sensors. To more precisely interpret observed sensor data in terms of the underlying brain activity, it is possible to reconstruct brain activity from MEG data. Reconstruction of brain activity from MEG data typically involves two major components—a forward model and an inverse model.

#### ***3.1 Forward Models Describing Brain Activity and Measurements***

The forward model consists of three sub-components—a source model, a volume conductor, and a measurement model. Typical source models assume that the MEG measurements outside the head are generated primarily by electric current dipoles located in the brain. This model is consistent with available measurements of coherent synaptic and intracellular currents in cortical columns that are thought to be major contributors to MEG and EEG signals. Although several more

complex source models have been proposed recently, the equivalent current dipole is still the dominant source model in the literature (Jerbi et al. 2002; Mosher et al. 1999b; Nolte and Curio 2000; von Ellenrieder et al. 2005). Given the distance between the sources in the brain and the sensors outside the head, the dipole is still a reasonable approximation of the sources.

Volume conductor models refer to the equations that govern the relation between the source model and the sensor measurements—i.e. the electric potentials or the magnetic fields. These surface integral equations, obtained by solving Maxwell's equations under quasi-static conditions, can be solved analytically for special geometries of the volume conductor, such as a sphere and ellipsoids. For realistic volume conductors, various numerical techniques such as finite-element and boundary-element methods are employed. These methods are very time consuming and their use may appear impractical in many settings because of the lack of knowledge about specific parameters used in these models (Mosher et al. 1999b).

Measurement models refer to the specific measurement systems used in EEG and MEG including the position of the sensors relative to the head. For instance, different MEG systems measure axial versus planar gradients of the magnetic fields with respect to different locations of reference sensors. The measurement model incorporates such information about the type of measurement and the geometry of the reference sensors. Since MEG sensor arrays are fixed relative to the head of a subject, it is necessary to measure the position of head relative to the sensor array. Typically this is accomplished by attaching head-localization coils to fiducial landmarks on the scalp, passing current through these coils, measuring the magnetic field created by the currents passed, and triangulating to locate the head-position relative to the sensor array. In many MEG systems, head localization is accomplished every 5–10 min because it disrupts normal data collection. Within a block of 10 min, with subjects in a supine position with their heads securely positioned in the array, typically head-movements are found to be less than 5 mm. However, more modern systems are sometimes equipped with continuous head-localization procedures that enable constant updating of sensor locations relative to the head and also correction for subjects' head movements.

The source, volume conductor and measurement models are typically combined and embodied in the idea called the “forward-field” that describes a linear relationship between sources and the measurements. Usually, we assume that the forward-field matrix is known. We can easily calculate the forward field for equivalent electric current dipoles in a spherical volume conductor model for a whole-head axial gradiometer MEG system. In this model, MEG is sensitive only to the tangential component of the primary current dipoles, whereas EEG is sensitive to all components but sensitive to uncertainties in the head model. Simultaneous MEG and EEG can be acquired in most modern MEG systems and require some modification to the forward-field matrix for combined MEG/EEG measurements especially for more realistic source, volume conductor and measurement models.

Co-registration is an integral part of forward model construction. Co-registration involves defining three fiducial points on an individual subject's head surface, which creates a coordinate system that includes the brain and the position of the MEG sensors relative to it. Based on these fiducial landmarks, a transformation matrix is obtained that enables co-registration with the subjects MRI. This allows for the source locations and sensors to be defined in MRI coordinates and enables interpretation of inverse model reconstructions in terms of the underlying brain anatomy provided by MRI.

### ***3.2 Identifying and Reducing Influences from Sources of Noise in MEG***

An enduring problem in MEG-based imaging is that the brain responses to sensory or cognitive events is small when compared to the large number of sources of noise, artifacts (biological and non-biological) and interference from spontaneous brain activity unrelated to the sensory or cognitive task of interest. All existing methods for brain source localization are hampered by these many sources of noise present in MEG data. For example, the magnitude of the stimulus-evoked auditory cortical sources are on the order of noise on a single trial, and so typically 75–200 averaged trials are at least needed in order to clearly distinguish the sources above noise. This limits the type of questions that can be asked, and is prohibitive for examining processes such as learning that can occur over just one or several trials. Averaging across trials is time-consuming and therefore difficult for a subject or patient to hold still or pay attention through the duration of the experiment. Gaussian thermal noise or Gaussian electrical noise is also present at the MEG or EEG sensors themselves. Background room interference from power lines and electronic equipment, for example, can be problematic. Biological noise such as heartbeat, eye blink or other muscle artifact can also be present. Ongoing brain activity itself, including the drowsy-state alpha ( $\sim 10$  Hz) rhythm can drown out evoked brain sources.

Noise in MEG and EEG data is typically reduced by a variety of preprocessing algorithms before being used by source localization algorithms. Simple forms of preprocessing include filtering out frequency bands not containing a brain signal of interest. Additionally and more recently, Independent Component Analysis (ICA) (Delorme and Makeig 2004; Makeig et al. 1997) as well as other blind source separate methods (Parra et al. 2002, 2005; Tang et al. 2002a, b) have been used to remove artifactual components, such as eye blinks. More sophisticated techniques have also recently been developed using graphical models for preprocessing prior to source localization (Nagarajan et al. 2006, 2007). Therefore, algorithms for source localization from MEG and EEG data typically use a two-stage procedure—the first for noise/interference removal and the second for source localization. However, more recent algorithms that integrate interference suppression with source reconstructions have also been proposed and provide for robust source reconstruction (Wipf et al. 2010; Zumer et al. 2007).

## 4 Inverse Algorithms for Magnetoencephalographic Imaging

Inverse algorithms are used to solve the bioelectromagnetic inverse problem i.e. estimating neural source model parameters from MEG and EEG measurements obtained outside the human head. In general, there are no unique solutions to the inverse problem because there are many source configurations that could result in the sensor observations, even in the absence of noise and infinite spatial or temporal sampling. This non-uniqueness is referred to as the ill-posed nature of the inverse problem. Nevertheless, to get around this non-uniqueness, various estimation procedures incorporate prior knowledge and constraints about source characteristics such as possible source locations, the source spatial extent, the total number of sources or the source frequency/time-frequency characteristics.

Inverse algorithms can be broadly classified into two categories—parametric dipole fitting and non-parametric whole-brain imaging methods. Parametric dipole fitting methods assume that a small set of current dipoles (usually 2–5) can adequately represent some unknown source distribution. In this case, the dipole locations and moments form a set of unknown parameters which are typically found using either a non-linear least square fit or multiple signal classification algorithms (MUSIC) or maximum likelihood estimation methods (Mosher et al. 1999a). Parametric dipole fitting has been successfully used clinically for localization of early sensory responses in somatosensory and auditory cortices. Figure 1 shows an example of parametric dipole localization in the context of somatosensory evoked responses, and shows that responses to early somatosensory peaks can often be localized to activity arising from primary somatosensory cortex located in the central sulcus.

Two major problems exist in dipole fitting procedures. First, due to non-linear optimization there are problems of local minima when more than two dipole parameters are estimated and this is usually manifested by sensitivity to initialization (Huang et al. 1998). Brute-force search methods have a huge computational burden—exponential in the number of parameters (Mosher et al. 1992, 1993). A second, more difficult problem in parametric methods is that often these methods require a priori knowledge of the number of dipoles. Often, such information about model order is not known a priori, especially for complex brain mapping conditions, and the resulting localization of higher-order cortical functions can sometimes be unreliable. Although information theoretic or Bayesian estimation criteria have been proposed to address this problem, the success of these approaches is less clear as these are not widely used (Campi et al. 2011; Kiebel et al. 2008; Sorrentino et al. 2009; Wolters et al. 1999). Nevertheless, many basic neuroscience and clinical studies to date have successfully used dipole-fitting procedures to gain important insights (Aine et al. 2010; Salmelin et al. 1994; Susac et al. 2009).

Non-parametric whole brain imaging is an alternative approach to estimate the inverse problem. The relevant localization problem can be posed as follows. The measured signal is a  $d_b \times n$  matrix  $B$ , where  $d_b$  equals the number of sensors and

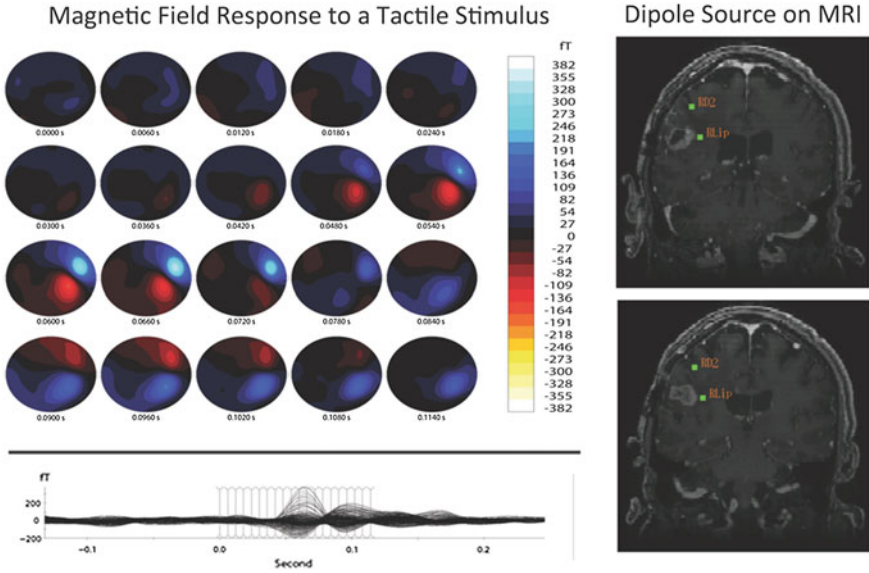


**Fig. 1** Example case of parametric dipole localization of separate somatosensory stimulation of the right lip (RLip) and right index finger (RD2). Multiple stimulus trials are performed for each skin stimulation site during MEG recordings. The trials are averaged and a single dipole is reconstructed for each site using the non-linear fit method. The resulting dipoles are then displayed on a co-registered, T1-weighted post-gadolinium coronal MR slice

$n$  is the number of time points at which measurements are made and the unknown sources are given by a  $d_s \times n$  matrix  $S$  which is the (discretized) amplitude of the source activity at  $d_s$  candidate locations obtained from the forward model calculations. In this case,  $B$  and  $S$  are related by the generative model

$$B = LS + E$$

where  $L$  is the composite forward-field matrix that captures the relationship between unit sources all over the brain and the expected pattern of magnetic field measurement on the sensor array. The number of candidate source locations is much larger than the number of sensors ( $d_s \gg d_b$ ). Therefore, the problem reduces to estimation of the activity in each source regions, which are reflected by the non-zero rows of the source estimate matrix  $\hat{S}$ .  $E$  is a noise or interference term discussed earlier.

Many whole-brain imaging algorithms impose constraints on source locations i.e. the candidate locations for sources based on anatomical and functional information obtained from other brain imaging modalities. Such constraints within a Bayesian framework are embedded in a prior distribution  $p(S)$  either implicitly or explicitly. If under a given experimental or clinical paradigm this  $p(S)$  were



somehow known exactly, then the posterior distribution can be computed via Bayes rule:

$$p(S|B) = p(B|S)p(S)/p(B).$$

This distribution contains all possible information about the unknown  $S$  conditioned on the observed data  $B$ . Two fundamental problems prevent using  $p(S|B)$  for source localization. First, for most priors  $p(S)$ , the normalization distribution  $p(B)$  given by

$$p(B) = \int p(B|S)p(S)ds$$

cannot be computed analytically. If only a point estimate for  $S$  is desired, rather than a full distribution, then this normalizing distribution may not be needed. For example, a popular estimator is the minimum-norm estimator which involves finding the value of  $S$  by assuming that prior  $p(S)$  has a Gaussian distribution with a single scalar variance term. This variance is related to the regularization constant in many implementations of the minimum-norm estimator and can be obtained by maximizing the posterior distribution (a.k.a. the MAP estimate) of  $p(S|B)$  which is invariant to  $p(B)$ . Second, and more importantly, we do not actually know the prior  $p(S)$  and so some appropriate distribution must be assumed, perhaps based on neurophysiological constraints or computational considerations. In fact, it is this choice, whether implicitly or explicitly specified, that differentiates a wide variety of localization methods (Phillips et al. 1997; Wipf and Nagarajan 2009).

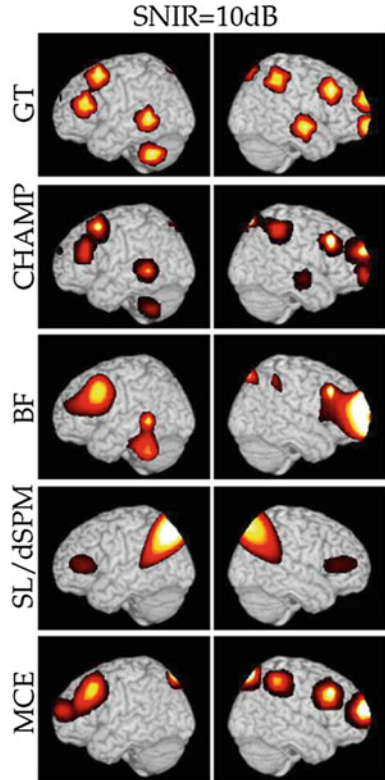
While seemingly quite different in many respects, we recently presented a generalized framework that encompasses different whole-brain imaging methods for source localization and points to intimate connections between algorithms. We showed that many seemingly disparate algorithms for source imaging can be unified using a hierarchical Bayesian modeling framework with a general form of prior distribution, called Gaussian scale mixture, with flexible covariance components, and two different types of inferential procedures. The wide variety of Bayesian source localization methods that fall under this framework can be differentiated by the following factors: (1) selection of covariance component regularization terms; (2) choice of initial covariance component set; (3) optimization method/update rules; and (4) approximation to the lower bound on the marginal likelihood of the data. Bayesian source localization methods demonstrate a number of surprising similarities or out-right equivalences between what might otherwise appear to be very different algorithms. Specifically, from the vantage point of a simple Gaussian scale mixture model with flexible covariance components, our initial work in this area analyzed and extended several broad categories of Bayesian inference directly applicable to source localization including empirical Bayesian approaches, standard MAP estimation, and variational Bayesian (VB) approximations. This perspective leads to explicit connections between many established algorithms and suggests natural extensions for handling unknown dipole orientations, extended

source configurations, correlated sources, temporal smoothness, and computational expediency. Specific imaging methods elucidated under this paradigm include weighted minimum L2-norm, FOCUSS, minimum-L1 norm (also called minimum-current estimation (MCE)), VESTAL, sLORETA, ReML and covariance component estimation, beamforming, Variational Bayes, and Automatic relevance determination (ARD) with multiple sparse priors (MSP). Perhaps surprisingly, all of these methods can be formulated as particular cases of covariance component estimation using different concave regularization terms and optimization rules, making general theoretical analyses and algorithmic extensions/improvements particularly relevant.

These ideas help to bring an insightful perspective to Bayesian source imaging methods, reduce confusion about how different techniques relate to one another, and expand the range of feasible applications. Additionally, there are numerous promising directions for future research, including time-frequency extensions, alternative covariance component parameterizations, and integration with robust interference suppression. These insights allow for continued development of novel algorithms for whole-brain imaging in relation to prior efforts in this enterprise. Figure 2 shows performance in simulations using one such novel algorithm, called Champagne, as well as reconstructions from popular benchmark algorithms for comparisons that highlight their poorer spatial resolution and sensitivity to correlated sources and noise (Owen et al. 2012; Wipf et al. 2010). When compared to ground-truth it can be seen that Champagne is the algorithm that is able to reconstruct the source configuration. Figure 3 shows source reconstructions of auditory evoked responses using called Champagne, and benchmarks algorithms. Auditory evoked responses are challenging datasets because of high degree of correlations between bilateral auditory cortices. In these real datasets from three different subjects, it can also be seen that Champagne is the only algorithm able to reliably reconstruct bilateral auditory cortical activity.

Instead of simultaneous estimation of all sources a popular alternative is to scan the brain and estimate source amplitude at each source location independently. It can be shown that such scanning methods are closely related to whole-brain imaging methods, and the most popular scanning algorithms are adaptive spatial filtering techniques, more commonly referred to as “adaptive beamformers” or just “beamformers” (Sekihara and Nagarajan 2008). Adaptive beamformers have been shown to be quite simple to implement and are powerful techniques for characterizing cortical oscillations and are closely related to other whole-brain imaging methods. However, one major problem with adaptive beamformers is that they are extremely sensitive to the presence of strongly correlated sources. Although they are robust to moderate correlations, in the case of auditory studies, since auditory cortices are largely synchronous in their activity across the two hemisphere, these algorithms tend to perform poor for auditory evoked datasets (without workarounds), and many modifications have been proposed for reducing the influence of correlated sources (Dalal et al. 2006). The simplest such work-around is to use half the sensors corresponding to each hemisphere separately, and this approach works surprisingly well for cross-hemispheric interactions. Other

**Fig. 2** Localization performance in simulations. A single example of the localization results for 10 clusters (each with 10 dipoles) at SNIR = 10 dB with the vector lead field and real brain-noise. The ground truth (*GT*) location of the clusters are shown for comparison, first *row*. The results with Champagne (*CHAMP*) are shown in the second *row* and the comparison algorithms, minimum-variance adaptive beamformer (*BF*), sLORETA or dSPM (*SL/dSPM*), and generalized minimum-current estimation (*MCE*) are shown in the subsequent *rows*. We project the source power to the surface of a template brain



modifications to the original algorithms have been proposed in the literature that require some knowledge about the location of the correlated source region (Dalal et al. 2006; Quraan and Cheyne 2010). Recently, we have shown that significant improvements in performance can be achieved by modern Bayesian inference algorithms that are closely related to minimum-variance adaptive beamformers and these extensions allow for accurate reconstructions of a large number of sources from typical configurations of MEG sensors (Wipf et al. 2010; Zumer et al. 2007, 2008).

## 5 Temporal and Spatial Resolution of MEG Imaging

Since MEG data can be acquired at sub-millisecond time-scale, temporal resolution of MEG imaging is only limited by the sampling rate, typically  $\sim 1$  kHz, and in principle, cortical oscillations can be observed up to 500 Hz. In contrast to its temporal resolution, determining the spatial resolution of MEG imaging is challenging because it is highly dependent on the reconstruction algorithm chosen, as

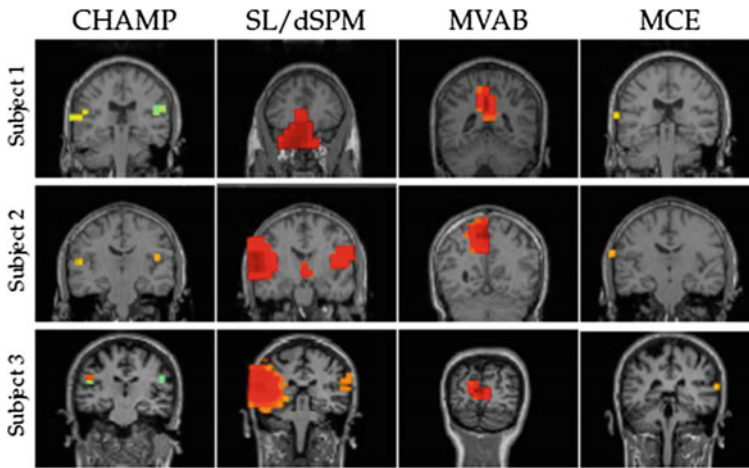


**Fig. 3** Auditory evoked field results for 3 subjects for four different benchmark algorithms. Champagne is able to reliably reconstruct bilateral auditory cortex activity in all subjects. SLORETA is only able to do so in two of the three subjects. MVAB fails because of the high-degree of correlations between the two sources. MCE is another sparse reconstruct algorithm that only finds auditory cortex in one hemisphere in each subject

well as a variety of factors such as signal-to-noise and interference-ratio, model formulation, forward-model accuracy, co-registration errors and accuracy of priors (Owen et al. 2012; Wipf et al. 2010). In general, it can be easily shown that the spatial resolution of MEG reconstruction is not limited by sensor spacing, because many adaptive methods can perform better than estimates based on spatial sampling criteria. For instance, while sensor spacing in many axial gradiometer systems is 2.2 cm, reconstruction accuracy can in some cases be as small as 3 mm! In general, co-registration errors alone can be on the order of 3 mm (Roberts et al. 2000). While whole-brain imaging algorithms, such as minimum-norm methods, have poor spatial resolution on the order of a few centimeters, the spatial resolution of adaptive spatial filtering methods, and more recent whole-brain reconstruction methods based on machine learning techniques, are difficult to generally compute because these estimates depend on the data and factors contributing to data quality etc. As a rule of thumb, for typical datasets, these newer methods can reconstruct tens-to-hundreds of sources about 0.5 cm apart (assuming time-frequency separation and detectability) and this can be considered an approximate spatial resolution for MEG, keeping in mind that under certain circumstances the spatial resolution can be even greater (Owen et al. 2012; Wipf et al. 2010).

A common myth, related to the spatial resolution of MEG, is its lack of sensitivity to gyral crown activity and relative insensitivity to deep sources. While it is a fact that for single spherical volume conductor models MEG sensors are insensitive to radially pointing dipoles, this does not necessarily translate to gyral sources. It has been shown that, using realistic volume conductor models (such as

boundary element methods or multiple local-sphere models), some sensitivity to radial sources can be recovered, and that there is no predominant loss of sensitivity to gyral sources (Hillebrand and Barnes 2002). Furthermore, while there is a significant drop in sensitivity to deeper sources because their contributions will fall by approximately the square of the distance to the sensors, recovery of deep sources is an issue of the signal to noise ratio. In general, if high signal-to-noise ratio data are recorded, there is no inherent problem in recovery of deep sources with some of the newer Bayesian reconstruction methods. However, mid-brain sources have two additional problems. First, they may not have dipolar organization due to the architectures and second, the uncertainties in the lead-field increases for deep brain sources, thereby making them more difficult to reconstruct.

## **6 From Single Subject Reconstructions to Group Level Inference**

While the power of MEG imaging is its ability to reconstruct the timing of activation across different frequency bands in single subjects, inferences across subjects require group level statistical analyses (Dalal et al. 2008). The most ubiquitous form of group analysis of MEG studies of auditory cortex are based on parameters, obtained from dipole fitting of typical component peaks in the response, such as timing, amplitude, location and sometimes orientation. For the less common whole-brain imaging and scanning based algorithms, group analysis of data across subjects have typically paralleled similar procedures for whole-brain analysis based on fMRI and PET studies (Singh et al. 2003, 2002). These procedures include spatial normalization to template brains, general-linear modeling of experimental effects, parametric and non-parametric inference procedures, and corrections for multiple comparisons. It is to be noted that group level statistical corrections for multiple comparisons are not yet as well developed for MEG imaging studies as they are for fMRI, and fMRI correction procedures such as family wise error FWE can sometimes be too conservative for MEG reconstructions for a variety of reasons, including the fact that spatial correlations in reconstructed images are higher than in fMRI (Dalal et al. 2008; Darvas et al. 2004; Owen et al. 2012).

## **7 From Source Activity Imaging to Functional Connectivity Imaging**

It is now well recognized in systems and cognitive neuroscience that it is necessary to examine not only activity within an area during an active or inactive state, but also how the brain integrates information *across* multiple regions. The term

functional connectivity essentially defines the complex functional interaction between local and more remote brain areas. Although a common approach is to examine functional connectivity by using hemodynamic measures of brain activity (such as fMRI), MEG directly measures changes in the magnetic field induced by underlying neuronal currents, and is better suited for modeling these types of interactions. Decomposition of information across, space, time, and oscillatory domains yields complex information about how sources in the brain interact across many levels.

Despite the advantage of MEG (and EEG) in the temporal domain over fMRI, there have been relatively few publications that assess event-related or resting-state functional connectivity using MEG or EEG as compared to fMRI. There are two genres of metrics used in MEG functional connectivity: bivariate quantities are calculated in a pair-wise fashion between pairs of voxels and multivariate techniques model the interactions between several regions of interest. Likewise, functional connectivity metrics in MEG data analyses can be applied either in sensor-space or in source-space. Although many metrics have been proposed for functional connectivity in MEG, no careful comparisons have been made for the same dataset across bivariate and multivariate metrics.

### ***7.1 Bivariate Metrics of Functional Connectivity in MEG***

Bivariate metrics can be applied to MEG/EEG data in two ways. Since these metrics are computed between two time courses, they can either be computed between target sensors/voxels or they can be computed between all sensors/voxels and then an average connectivity value can be calculated for every sensor/voxel. The first of these methods is used when there is knowledge about the areas involved and can be considered a “hypothesis-driven” approach. The second, in contrast, can be described as a “data-driven” approach and is applicable when there is not a priori knowledge about which areas should exhibit high or changed connectivity. Correlation and its frequency domain analog, coherence, are the two most commonly used bivariate metrics in the literature (Nunez et al. 1997). An extension of using coherence on sensor time courses, a source localization algorithm called DICS, is particularly designed to construct coherent activity by estimating time course and calculating magnitude coherence (Gross et al. 2001). There are also phase difference-based bivariate metrics that can be applied in similar fashion to the metrics described above. The difference in instantaneous phase between two time courses can be calculated using the Hilbert transform. There are different subsequent calculations that can be performed with the phase difference, e.g. phase coherence (PC), phase synchronization, index of synchronization.

All types of bivariate metrics are susceptible to spurious interactions that arise from volume conduction artifacts in MEG and EEG recordings. The magnetic field or electric potential generated by a single neuronal source is picked up by not only the nearest sensor to the source, but the neighboring sensors also pick up the signal

with a zero-time lag. This creates instantaneous blurring across the sensors. As such, the time courses of many sensors can contain overlapping information due to this electromagnetic phenomenon, which can produce spurious interactions. Some bivariate metrics used for MEG and EEG functional connectivity analyses have been designed to overcome this blurring by isolating the non-zero-time-lag interactions from the zero-time-lag interactions, namely imaginary coherence (IC) and phase lag index (PLI). Both metrics are designed to assess only non-zero time lagged interactions in source or sensor data in order to cancel out the effects of cross-talk across the detection sensors.

Imaginary coherence is calculated by only considering the imaginary component of the complex-valued coherence. The imaginary part of the coherence is produced by non-instantaneous interactions between waveforms. It was found to be a better measure of coupling than the magnitude of coherence in an EEG experiment of voluntary finger movement (Nolte et al. 2004). PLI is similar to IC in that it includes only information that is transmitted at a non-zero time lag; any two signals that are instantaneously coupled and therefore have a phase difference of zero, are not included in the calculation of PLI. PLI and PC of EEG and MEG data were more sensitive than IC to increasing levels of true synchronization in the simulated data, but IC and PLI were less susceptible to spurious correlations in the data due to common sources (Stam et al. 2007). In addition, PLI and IC were better able to detect beta band connectivity and uncovered a different spatial pattern of connectivity in the MEG data. IC has also revealed significant changes in the over all resting-state connectivity induced by brain lesions (de Pasquale et al. 2010, 2012; Guggisberg et al. 2007; Martino et al. 2011; Marzetti et al. 2013; Tarapore et al. 2012; Hipp et al. 2011, 2012) (Fig. 4).

## ***7.2 Multivariate Connectivity Metrics in MEG***

In contrast to bivariate metrics, which compute relationships between elements in a pair-wise fashion, multivariate metrics are able to model interactions between multiple areas in a single model (Astolfi et al. 2005). While powerful, computational complexity is an issue when performing a multivariate analysis. While all areas can be modeled simultaneously, the limitation of these methods lies in maintaining the necessary condition that the number of parameters fit in the model does not exceed the number of time points. This is done by considering fewer areas or voxels or by limiting the number of lags the model will analyze. Multivariate autoregressive models (MVAR) can be applied in the time domain, or in the frequency domain, as is the case with partial directed coherence and direct transfer function methods. Although some of these methods have been demonstrated to be powerful in determining neural networks associated with basic sensory processing (Porcaro et al. 2009). Future studies will determine how these metrics can be extended to examinations of impairments in cognitive function in a variety of clinical populations.



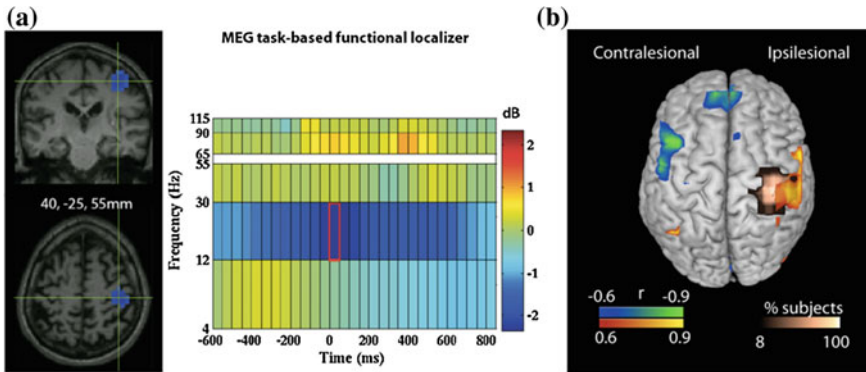


**Fig. 4** Activation and Functional Connectivity in Stroke. **a** Activation of motor cortex and its associated time-frequency plot of the voxel of maximal power change in the beta frequency band during affected finger button press. **b** Results of the correlation analysis between baseline resting MEGI functional connectivity and recovery scores. *Gold* indicates the location of the lesion and activated motor cortex. *Blue* indicates negative correlations. *Red* indicates positive correlations. Strong ipsilesional connectivity predicts recovery (Westlake et al. 2012)

Nevertheless, already in these early days of functional connectivity analyses, it has been shown to have profound clinical significance as disturbances in networks as manifested as abnormalities in functional connecting even during resting state. Recent studies have shown this to be the case in many clinical conditions such as brain tumor, schizophrenia, stroke, and developmental disorders (Bartolomei et al. 2006a, b; Bosma et al. 2008a, b). For example, neurocognitive effects are correlated with functional connectivity changes in brain tumor patients, especially in patients with low-grade gliomas (Douw et al. 2008, 2009, 2010; van Dellen et al. 2012). Similarly, combining activation mapping and resting-state functional connectivity can help predict functional recovery in stroke. Therefore, mapping functional connectivity and combining this information with brain activation studies may be an important component in surgical planning and clinical diagnosis in a variety of disorders (Martino et al. 2011; Tarapore et al. 2012).

## 8 Conclusions

Great strides have occurred in the development of novel and powerful algorithms for MEG imaging. These algorithmic approaches not only enable more accurate reconstruction of brain activity, their time courses and spectral power fluctuations, but also enable us to examine functional connectivity between different brain regions from MEG data. These efforts pave the way novel and powerful applications for MEG imaging in many basic and clinical neuroscience studies of neural oscillations in the human brain.



## References

- Aine CJ, Bryant JE, Knoefel JE, Adair JC, Hart B, Donahue CH, Montano R, Hayek R, Qualls C, Ranken D, Stephen JM (2010) Different strategies for auditory word recognition in healthy versus normal aging. *Neuroimage* 49:3319–3330
- Astolfi L, Cincotti F, Mattia D, Babiloni C, Carducci F, Basilisco A, Rossini PM, Salinari S, Ding L, Ni Y, He B, Babiloni F (2005) Assessing cortical functional connectivity by linear inverse estimation and directed transfer function: simulations and application to real data. *Clin Neurophysiol* 116:920–932
- Bartolomei F, Bosma I, Klein M, Baayen JC, Reijneveld JC, Postma TJ, Heimans JJ, Van Dijk BW, De Munck JC, De Jongh A, Cover KS, Stam CJ (2006a) Disturbed functional connectivity in brain tumour patients: evaluation by graph analysis of synchronization matrices. *Clin Neurophysiol* 117:2039–2049
- Bartolomei F, Bosma I, Klein M, Baayen JC, Reijneveld JC, Postma TJ, Heimans JJ, Van Dijk BW, De Munck JC, De Jongh A, Cover KS, Stam CJ (2006b) How do brain tumors alter functional connectivity? A magnetoencephalography study. *Ann Neurol* 59:128–138
- Belliveau JW, Kwong KK, Kennedy DN, Baker JR, Stern CE, Benson R, Chesler DA, Weisskoff RM, Cohen MS, Tootell RB et al (1992) Magnetic resonance imaging mapping of brain function. Human visual cortex. *Invest Radiol* 27(Suppl 2):S59–S65
- Bosma I, Douw L, Bartolomei F, Heimans JJ, Van Dijk BW, Postma TJ, Stam CJ, Reijneveld JC, Klein M (2008a) Synchronized brain activity and neurocognitive function in patients with low-grade glioma: a magnetoencephalography study. *Neuro Oncol* 10:734–744
- Bosma I, Stam CJ, Douw L, Bartolomei F, Heimans JJ, Van Dijk BW, Postma TJ, Klein M, Reijneveld JC (2008b) The influence of low-grade glioma on resting state oscillatory brain activity: a magnetoencephalography study. *J Neurooncol* 88:77–85
- Campi C, Pascarella A, Sorrentino A, Piana M (2011) Highly automated dipole estimation (HADES). *Comput Intell Neurosci* 2011:982185
- Dalal SS, Guggisberg AG, Edwards E, Sekihara K, Findlay AM, Canolty RT, Berger MS, Knight RT, Barbaro NM, Kirsch HE, Nagarajan SS (2008) Five-dimensional neuroimaging: localization of the time-frequency dynamics of cortical activity. *Neuroimage* 40:1686–1700
- Dalal SS, Sekihara K, Nagarajan SS (2006) Modified beamformers for coherent source region suppression. *IEEE Trans Biomed Eng* 53:1357–1363
- Darvas F, Pantazis D, Kucukaltun-Yildirim E, Leahy RM (2004) Mapping human brain function with MEG and EEG: methods and validation. *Neuroimage* 23(Suppl 1):S289–S299
- De Pasquale F, Della Penna S, Snyder AZ, Lewis C, Mantini D, Marzetti L, Belardinelli P, Ciancetta L, Pizzella V, Romani GL, Corbetta M (2010) Temporal dynamics of spontaneous MEG activity in brain networks. *Proc Natl Acad Sci U S A* 107:6040–6045
- De Pasquale F, Della Penna S, Snyder AZ, Marzetti L, Pizzella V, Romani GL, Corbetta M (2012) A cortical core for dynamic integration of functional networks in the resting human brain. *Neuron* 74:753–764
- Delorme A, Makeig S (2004) EEGLAB: an open source toolbox for analysis of single-trial EEG dynamics including independent component analysis. *J Neurosci Methods* 134:9–21
- Douw L, Baayen H, Bosma I, Klein M, Vandertop P, Heimans J, Stam K, De Munck J, Reijneveld J (2008) Treatment-related changes in functional connectivity in brain tumor patients: a magnetoencephalography study. *Exp Neurol* 212:285–290
- Douw L, Baayen JC, Klein M, Velis D, Alpherts WC, Bot J, Heimans JJ, Reijneveld JC, Stam CJ (2009) Functional connectivity in the brain before and during intra-arterial amobarbital injection (Wada test). *Neuroimage* 46:584–588
- Douw L, Van Dellen E, Baayen JC, Klein M, Velis DN, Alpherts WC, Heimans JJ, Reijneveld JC, Stam CJ (2010) The lesioned brain: still a small-world? *Front Hum Neurosci* 4:174
- Gross J, Kujala J, Hamalainen M, Timmermann L, Schnitzler A, Salmelin R (2001) Dynamic imaging of coherent sources: studying neural interactions in the human brain. *Proc Natl Acad Sci U S A* 98:694–699

- Guggisberg AG, Honma SM, Findlay AM, Dalal SS, Kirsch HE, Berger MS, Nagarajan SS (2007) Mapping functional connectivity in patients with brain lesions. *Ann Neurol* 63(2):193–203
- Hillebrand A, Barnes GR (2002) A quantitative assessment of the sensitivity of whole-head MEG to activity in the adult human cortex. *Neuroimage* 16:638–650
- Hipp JF, Engel AK, Siegel M (2011) Oscillatory synchronization in large-scale cortical networks predicts perception. *Neuron* 69:387–396
- Hipp JF, Hawellek DJ, Corbetta M, Siegel M, Engel AK (2012) Large-scale cortical correlation structure of spontaneous oscillatory activity. *Nat Neurosci* 15:884–890
- Huang M, Aine CJ, Supek S, Best E, Ranken D, Flynn ER (1998) Multi-start downhill simplex method for spatio-temporal source localization in magnetoencephalography. *Electroencephalogr Clin Neurophysiol* 108:32–44
- Jerbi K, Mosher JC, Baillet S, Leahy RM (2002) On MEG forward modelling using multipolar expansions. *Phys Med Biol* 47:523–555
- Kiebel SJ, Daunizeau J, Phillips C, Friston KJ (2008) Variational Bayesian inversion of the equivalent current dipole model in EEG/MEG. *Neuroimage* 39:728–741
- Logothetis NK, Pauls J, Augath M, Trinath T, Oeltermann A (2001) Neurophysiological investigation of the basis of the fMRI signal. *Nature* 412:150–157
- Makeig S, Jung TP, Bell AJ, Ghahremani D, Sejnowski TJ (1997) Blind separation of auditory event-related brain responses into independent components. *Proc Natl Acad Sci U S A* 94:10979–10984
- Martino J, Honma SM, Findlay AM, Guggisberg AG, Owen JP, Kirsch HE, Berger MS, Nagarajan SS (2011) Resting functional connectivity in patients with brain tumors in eloquent areas. *Ann Neurol* 69:521–532
- Marzetti L, Della Penna S, Snyder AZ, Pizzella V, Nolte G, De Pasquale F, Romani GL, Corbetta M (2013) Frequency specific interactions of MEG resting state activity within and across brain networks as revealed by the multivariate interaction measure. *Neuroimage* 79:172–183
- Mosher JC, Baillet S, Leahy RM (1999a) EEG source localization and imaging using multiple signal classification approaches. *J Clin Neurophysiol* 16:225–238
- Mosher JC, Leahy RM, Lewis PS (1999b) EEG and MEG: forward solutions for inverse methods. *IEEE Trans Biomed Eng* 46:245–259
- Mosher JC, Lewis PS, Leahy RM (1992) Multiple dipole modeling and localization from spatio-temporal MEG data. *IEEE Trans Biomed Eng* 39:541–557
- Mosher JC, Spencer ME, Leahy RM, Lewis PS (1993) Error bounds for EEG and MEG dipole source localization. *Electroencephalogr Clin Neurophysiol* 86:303–321
- Nagarajan SS, Attias HT, Hild KE 2nd, Sekihara K (2006) A graphical model for estimating stimulus-evoked brain responses from magnetoencephalography data with large background brain activity. *Neuroimage* 30:400–416
- Nagarajan SS, Attias HT, Hild KE 2nd, Sekihara K (2007) A probabilistic algorithm for robust interference suppression in bioelectromagnetic sensor data. *Stat Med* 26(21):3886–3910
- Niessing J, Ebisch B, Schmidt KE, Niessing M, Singer W, Galuske RA (2005) Hemodynamic signals correlate tightly with synchronized gamma oscillations. *Science* 309:948–951
- Nolte G, Bai O, Wheaton L, Mari Z, Vorbach S, Hallett M (2004) Identifying true brain interaction from EEG data using the imaginary part of coherency. *Clin Neurophysiol* 115:2292–2307
- Nolte G, Curio G (2000) Current multipole expansion to estimate lateral extent of neuronal activity: a theoretical analysis. *IEEE Trans Biomed Eng* 47:1347–1355
- Nunez PL, Srinivasan R (2006) A theoretical basis for standing and traveling brain waves measured with human EEG with implications for an integrated consciousness. *Clin Neurophysiol* 117:2424–2435
- Nunez PL, Srinivasan R, Westdorp AF, Wijesinghe RS, Tucker DM, Silberstein RB, Cadusca PJ (1997) EEG coherency. I: statistics, reference electrode, volume conduction, Laplacians, cortical imaging, and interpretation at multiple scales. *Electroencephalogr Clin Neurophysiol* 103:499–515

- Ogawa S, Tank DW, Menon R, Ellermann JM, Kim SG, Merkle H, Ugurbil K (1992) Intrinsic signal changes accompanying sensory stimulation: functional brain mapping with magnetic resonance imaging. *Proc Natl Acad Sci U S A* 89:5951–5955
- Owen JP, Wipf DP, Attias HT, Sekihara K, Nagarajan SS (2012) Performance evaluation of the Champagne source reconstruction algorithm on simulated and real M/EEG data. *Neuroimage* 60:305–323
- Parra L, Alvino C, Tang A, Pearlmutter B, Yeung N, Osman A, Sajda P (2002) Linear spatial integration for single-trial detection in encephalography. *Neuroimage* 17:223–230
- Parra LC, Spence CD, Gerson AD, Sajda P (2005) Recipes for the linear analysis of EEG. *Neuroimage* 28:326–341
- Phillips JW, Leahy RM, Mosher JC, Timsari B (1997) Imaging neural activity using MEG and EEG. *IEEE Eng Med Biol Mag* 16:34–42
- Porcaro C, Zappasodi F, Rossini PM, Tecchio F (2009) Choice of multivariate autoregressive model order affecting real network functional connectivity estimate. *Clin Neurophysiol* 120:436–448
- Quraan MA, Cheyne D (2010) Reconstruction of correlated brain activity with adaptive spatial filters in MEG. *Neuroimage* 49:2387–2400
- Roberts TP, Ferrari P, Perry D, Rowley HA, Berger MS (2000) Presurgical mapping with magnetic source imaging: comparisons with intraoperative findings. *Brain Tumor Pathol* 17:57–64
- Salmelin R, Hari R, Lounasmaa OV, Sams M (1994) Dynamics of brain activation during picture naming. *Nature* 368:463–465
- Sekihara K, Nagarajan SS (2008) Adaptive spatial filters for electromagnetic brain imaging. Springer, Heidelberg
- Singh KD, Barnes GR, Hillebrand A (2003) Group imaging of task-related changes in cortical synchronization using nonparametric permutation testing. *Neuroimage* 19:1589–1601
- Singh KD, Barnes GR, Hillebrand A, Forde EM, Williams AL (2002) Task-related changes in cortical synchronization are spatially coincident with the hemodynamic response. *Neuroimage* 16:103–114
- Sorrentino A, Parkkonen L, Pascarella A, Campi C, Piana M (2009) Dynamical MEG source modeling with multi-target Bayesian filtering. *Hum Brain Mapp* 30:1911–1921
- Stam CJ, Nolte G, Daffertshofer A (2007) Phase lag index: assessment of functional connectivity from multi channel EEG and MEG with diminished bias from common sources. *Hum Brain Mapp* 28:1178–1193
- Susac A, Ilmoniemi RJ, Pihko E, Nurminen J, Supek S (2009) Early dissociation of face and object processing: a magnetoencephalographic study. *Hum Brain Mapp* 30:917–927
- Tang AC, Pearlmutter BA, Malaszenko NA, Phung DB (2002a) Independent components of magnetoencephalography: single-trial response onset times. *Neuroimage* 17:1773–1789
- Tang AC, Pearlmutter BA, Malaszenko NA, Phung DB, Reeb BC (2002b) Independent components of magnetoencephalography: localization. *Neural Comput* 14:1827–1858
- Tank DW, Ogawa S, Ugurbil K (1992) Mapping the brain with MRI. *Curr Biol* 2:525–528
- Tarapore PE, Martino J, Guggisberg AG, Owen J, Honma SM, Findlay A, Berger MS, Kirsch HE, Nagarajan SS (2012) Magnetoencephalographic imaging of resting-state functional connectivity predicts postsurgical neurological outcome in brain gliomas. *Neurosurgery* 71:1012–1022
- Van Dellen E, Douw L, Hillebrand A, Ris-Hilgersom IH, Schoonheim MM, Baayen JC, De Witt Hamer PC, Velis DN, Klein M, Heimans JJ, Stam CJ, Reijneveld JC (2012) MEG network differences between low- and high-grade glioma related to epilepsy and cognition. *PLoS ONE* 7:e50122
- Von Ellenrieder N, Muravchik CH, Nehorai A (2005) MEG forward problem formulation using equivalent surface current densities. *IEEE Trans Biomed Eng* 52:1210–1217
- Vrba J, Robinson SE (2002) SQUID sensor array configurations for magnetoencephalography applications. *Supercond Sci Technol* 15:51–89

- Westlake KP, Hinkley LB, Bucci M, Guggisberg AG, Byl N, Findlay AM, Henry RG, Nagarajan SS (2012) Resting state alpha-band functional connectivity and recovery after stroke. *Exp Neurol* 237:160–169
- Wipf D, Nagarajan S (2009) A unified Bayesian framework for MEG/EEG source imaging. *Neuroimage* 44(3):947–966
- Wipf DP, Owen JP, Attias HT, Sekihara K, Nagarajan SS (2010) Robust Bayesian estimation of the location, orientation, and time course of multiple correlated neural sources using MEG. *Neuroimage* 49:641–655
- Wolters CH, Beckmann RF, Rienacker A, Buchner H (1999) Comparing regularized and non-regularized nonlinear dipole fit methods: a study in a simulated sulcus structure. *Brain Topogr* 12:3–18
- Zumer JM, Attias HT, Sekihara K, Nagarajan SS (2007) A probabilistic algorithm integrating source localization and noise suppression for MEG and EEG data. *Neuroimage* 37(1):102–115
- Zumer JM, Attias HT, Sekihara K, Nagarajan SS (2008) Probabilistic algorithms for MEG/EEG source reconstruction using temporal basis functions learned from data. *Neuroimage* 41:924–940